e-ISSN: 2689-4934

Available online at
http://uppp.uitm.edu.my/online-issues.html

ESTEEM Academic Journal Vol 22, September 2025, 92-105

ESTEEM
Academic Journal
(EAJ)

# A study on ZnO/GaN and ZnO/PGaN structures for optoelectronic applications via SILVACO TCAD

Nur Sabrina Mohd Hassan[1], Alhan Farhanah Abd Rahim[1*], Nurul Syuhadah Mohd Razali[1], Rosfariza Radzali[1], Ainorkhilah Mahmood[2], Irni Hamiza Hamzah[1], Zuraida Muhammad[1], Mohamed Fauzi Packeer Mohamed[3]

[1]*Faculty of Electrical Engineering, Universiti Teknologi MARA, Cawangan Pulau Pinang, 13500 Permatang Pauh, Penang, Malaysia*
[2]*Department of Applied Sciences, Universiti Teknologi Mara, Cawangan Pulau Pinang, 13500 Permatang Pauh, Penang, Malaysia*
[3]*School of Electrical and Electronic Engineering, Engineering Campus, Universiti Sains Malaysia, 14300 Nibong Tebal, Penang, Malaysia*

ARTICLE INFO

*Article history:*
Received 28 June 2025
Revised 18 August 2025
Accepted 5 September 2025
Online first
Published 15 September 2025

*Keywords:*
ZnO on GaN
ZnO on PGaN
Photocurrent
Dark current
Current gain
Silvaco
Photodetector

*DOI:*
10.24191/esteem.v21iSeptember.7129.g5014

ABSTRACT

The integration of metal oxide materials with semiconductor substrates has emerged as a promising strategy to enhance the performance of optoelectronic devices. However, studies focusing on zinc oxide (ZnO) embedded directly onto porous gallium nitride (PGaN) remain limited. This work aims to investigate the optoelectronic performance of ZnO on both GaN and PGaN substrates using SILVACO TCAD tools. ZnO layers with varying thicknesses (0.1 µm, 0.5 µm, and 1.0 µm) were simulated on GaN and two different pore diameters of PGaN (0.5 µm and 1.0 µm). Device structures were constructed and characterised for their dark current, illuminated current, and current gain. Results indicate that while the ZnO/GaN configuration exhibits higher photocurrent, the ZnO/PGaN structures demonstrate significantly enhanced current gain up to 12 times higher than non-porous counterparts. Notably, ZnO on 0.5 µm PGaN showed a higher photoresponse than that on 1.0 µm PGaN, highlighting the influence of pore diameter. It must be added that increasing the ZnO thickness led to improved photocurrent gain across all configurations. These findings suggest that both pore diameter and ZnO thickness critically influence the optical performance of ZnO/PGaN-based photodetectors.

[1*] Corresponding author. *E-mail address*: alhan570@uitm.edu.my
https://doi.org/10.24191/esteem.v21iSeptember.7129.g5014

## 1. INTRODUCTION

Zinc Oxide (ZnO) is a promising wide-bandgap semiconductor (3.28 eV) with a high exciton binding energy, making it attractive for ultraviolet (UV) photodetector applications [1]. However, the performance of ZnO-based devices is often restricted by its unstable p-type conductivity and relatively low light-absorption efficiency[1]. To overcome these limitations, researchers have explored ZnO heterojunctions with gallium nitride (GaN) [2], a direct wide-bandgap material (3.4 eV) known for its excellent electron mobility, chemical stability, and suitability for high-temperature operation[3, 4].

Recent studies have reported that ZnO/GaN heterojunctions exhibit enhanced optoelectronic responses, including improved photocurrent and faster response times [5, 6]. Nevertheless, the light-harvesting capability of these structures is constrained by the planar and dense nature of GaN substrates, which limits photon scattering and reduces the carrier-transport efficiency. To address this issue, porous GaN (PGaN) has emerged as a potential alternative due to its high surface area, tunable pore morphology, and the ability to act as a strain-relief buffer layer during epitaxial regrowth [7]. Porous architectures have been shown to significantly enhance light scattering, increase active surface area, and reduce dislocation densities, which are beneficial for photodetector applications [8-10]. Recent studies further confirmed these advantages, where nanoporous GaN layers demonstrated improved structural and optoelectronic properties due to the porosity-induced scattering [11], while advanced porous GaN nanopyramids enhanced the InGaN/GaN quantum well emission and internal quantum efficiency [12].

Several studies have demonstrated the integration of ZnO with porous GaN for improved sensing and photodetection. For instance, Wang et al.[8] reported that ZnO/PGaN heterojunctions exhibited enhanced humidity sensing due to increased surface states, while Wen et al. [13] highlighted the role of nanostructured GaN in improving carrier dynamics and responsivity in UV detectors. Ouyang et al.[10] further emphasised that charge-carrier engineering in porous and nanostructured oxide/semiconductor systems can significantly boost the photoelectric performance. However, most of these studies are experimental and focus on qualitative improvements, with limited attention given to the systematic evaluation of structural parameters such as pore diameter and ZnO thickness.

Despite progress in ZnO/GaN and ZnO/PGaN structures, comprehensive simulation-based studies investigating how pore geometry influences photocurrent gain and dark current remain scarce. In particular, the influence of pore diameter in modulating light scattering, carrier recombination, and device gain has not been fully clarified. This study, therefore, investigates ZnO on both GaN and porous GaN substrates using SILVACO TCAD tools, with emphasis on two pore diameters (0.5 μm and 1.0 μm) and ZnO thickness variations (0.1 μm, 0.5 μm, and 1.0 μm). The outcomes provide quantitative insights into the trade-off between pore size and ZnO thickness in optimising ZnO/PGaN photodetectors for enhanced sensitivity and reduced dark current.

## 2. METHODOLOGY

This study was conducted using SILVACO TCAD tools, comprising ATHENA for structure design and ATLAS for optical and electrical simulations. The simulation workflow is summarised in Fig. 1. The process began with defining the structure parameters and material choices in ATHENA, followed by structure construction in ATLAS, electrical simulation in TONYPLOT and analysis of the results.

https://doi.org/10.24191/esteem.v21iSeptember.7129.g5014

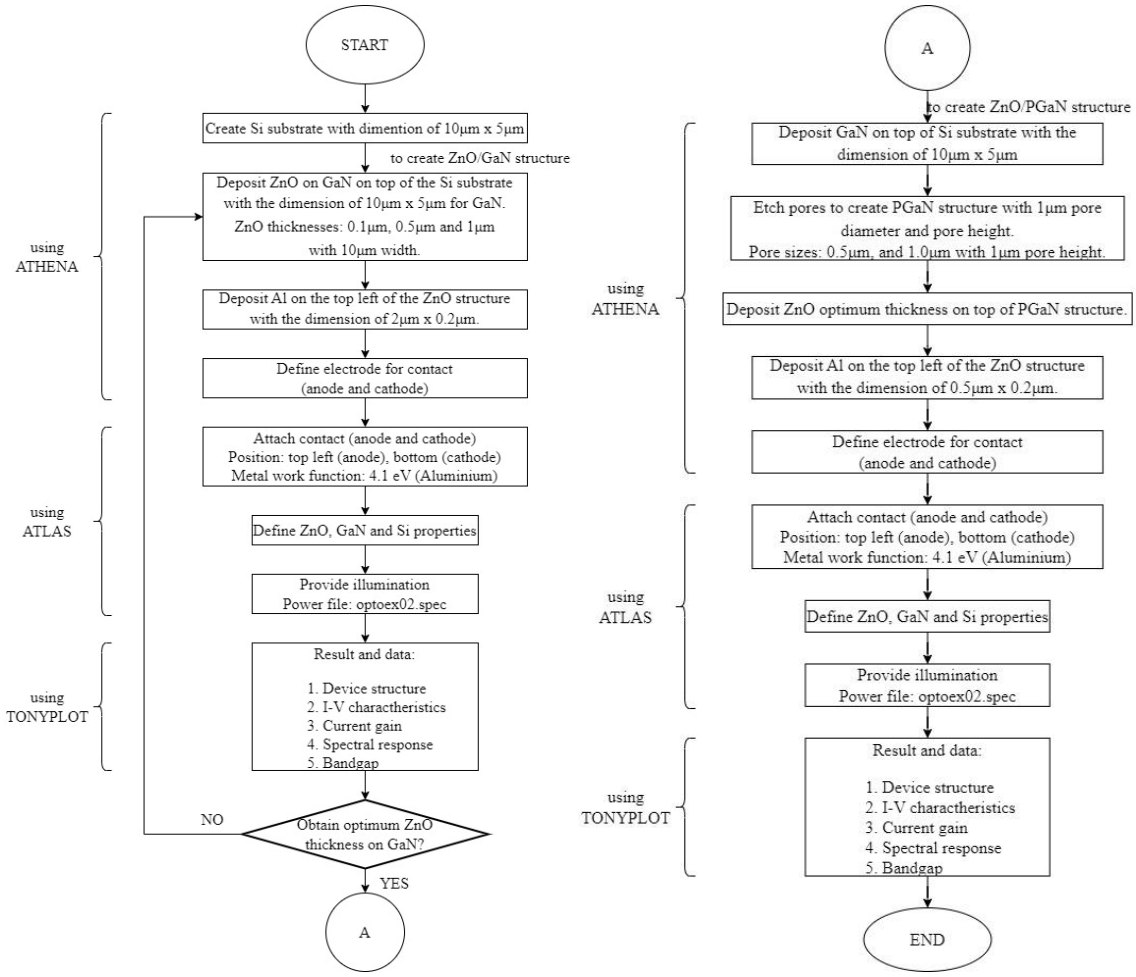


Fig 1. Flowchart of the project.

## 2.1 Device structure design using ATHENA

The device structure was built on a p-type silicon (p-Si) substrate (10 µm × 5 µm) doped with boron at a concentration of $1.8 \times 10^{16}$ $cm^{-3}$. A fine simulation mesh was applied, particularly in regions with high current flow to ensure numerical accuracy. An n-type GaN layer (5 µm) was deposited above the Si substrate, followed by an n-type ZnO layer with variable thicknesses (0.1 µm, 0.5 µm, and 1.0 µm). The ZnO layer underwent thermal annealing at 850 °C for 1 minute to activate dopants.

For porous configurations (ZnO/PGaN), cylindrical pores of 0.5 µm and 1.0 µm diameter (fixed depth of 2.0µm) were etched into the GaN layer before ZnO deposition. The pore diameters of 0.5 µm and 1.0 µm were selected as they fall within the typical range reported for electrochemically etched GaN structures [3, 7-8]. The 0.5 µm pores correspond to finer features that enhance the light scattering and surface-to-volume ratio, while 1.0 µm pores provide larger channels that influence the carrier transport and recombination. This comparison allows the evaluation of the trade-off between the scattering efficiency and structural porosity in ZnO/PGaN photodetectors. Aluminum (Al) electrodes (2 µm × 0.2 µm) were defined on the top-left (anode) and bottom (cathode) of the structure to complete the photodetector layout.

https://doi.org/10.24191/esteem.v21iSeptember.7129.g5014

## 2.2 Electrical and optical simulation in ATLAS

After defining the structure in ATHENA, it was imported into ATLAS for optical and electrical simulations. Key material parameters for ZnO, GaN, and Si such as bandgap energy, electron affinity, dielectric constant, carrier mobilities, and density of states were defined based on established literature [14-16]. These values, which are critical for an accurate simulation of electrical behaviour and carrier transport, are summarised in Table 1.

Table 1. Material properties used in ATLAS simulation [14-16].

| Parameters | ZnO | GaN | Si |
|---|---|---|---|
| Bandgap (eV) | 3.28 | 3.4 | 1.12 |
| Electron Affinity (eV) | 4.35 | 4.1 | 4.05 |
| Relative Permittivity, $\varepsilon_r$ | 8.12 | 8.9 | 11.8 |
| The density of States in the Conduction Band NC ($cm^{-3}$) | $2.2 \times 10^{18}$ | $2.3 \times 10^{18}$ | $2.8 \times 10^{19}$ |
| The density of States in the Valance Band NV ($cm^{-3}$) | $1.8 \times 10^{19}$ | $3.5 \times 10^{19}$ | $1.04 \times 10^{19}$ |
| Electron Mobility μn ($cm^2/Vs$) | 100 | 1800 | 1417 |
| Hole Mobility μp ($cm^2/Vs$) | 25 | 167 | 470 |

Recombination mechanisms, including Shockley–Read–Hall (SRH) and Auger recombination, were incorporated to reflect realistic carrier dynamics. Auger recombination is the mechanism by which an electron–hole pair recombines, transferring energy to a third free carrier [17]. If the third free carrier is an electron, it will either move toward a conduction band with a higher energy value or a valence band with a lower energy value. The Auger process is a three-body process requiring either one electron and two holes or two holes and one electron, and it reduces the photodetector's quantum efficiency because electron-hole recombination occurs without photon emission [9]. This model was defined in ATLAS prior to biasing the device. In addition, reducing the concentrations of external impurities and native defects can decrease the SRH recombination caused by the trapping of electrons by defect levels within the bandgap. The local carrier densities influence the rate of recombination in semiconductor bands and the principal occupancy state of the charge carriers [9]. The SRH recombination model is also included in the ATLAS device simulation. Optical illumination was then introduced using the BEAM statement, simulating a broadband light source spanning 0.3 μm to 0.7 μm. Simulations were run under both dark and illuminated conditions, with the voltage swept from 0 V to 5 V to extract I–V characteristics.

## 2.3 Design variations

The effect of structural variations on the device performance was analysed by varying the ZnO thickness and the PGaN pore diameter as shown in Table 2.

Table 2. Simulated device configuration.

| Structure | Pore Diameter (μm) | ZnO Thickness (μm) |
|---|---|---|
| ZnO/GaN | N/A | 0.1, 0.5, 1.0 |
| ZnO/PGaN | 0.5, 1.0 | 0.1, 0.5, 1.0 |

## 2.4 Data analysis

Simulation outputs were visualised and analysed using TONYPLOT. Extracted parameters included device structure profiles, doping distributions, I–V characteristics, spectral response, and photocurrent gain.

https://doi.org/10.24191/esteem.v21iSeptember.7129.g5014

Current gain was computed as the ratio of photocurrent ($I_p$) to dark current ($I_d$) under applied bias, as defined by Eq. (1):

$$Gain = \frac{Ip}{Id} \tag{1}$$

Fig. 2 illustrates the 2D cross-sectional morphology of both ZnO/GaN and ZnO/PGaN device structures designed in ATHENA, showing the substrate, active layers, and pore features.

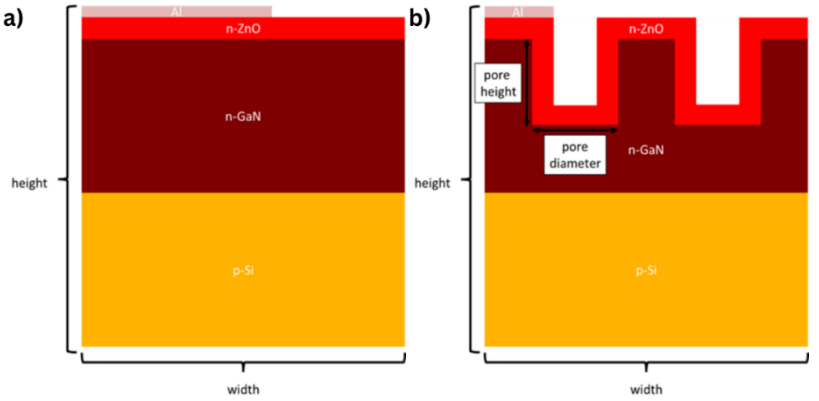


Fig 2. Cross-sectional morphology of designed devices using ATHENA a) ZnO/GaN photodetector structure on Si substrate. b) ZnO/PGaN structure showing etched pores in the GaN layer prior to ZnO deposition.

Fig. 3 illustrates the illumination setup and simulation configuration used in ATLAS. The light source is applied uniformly from the top surface to evaluate the device's photoresponse. This evaluation provides insight into how pore geometry and ZnO thickness influence the photodetector performance.

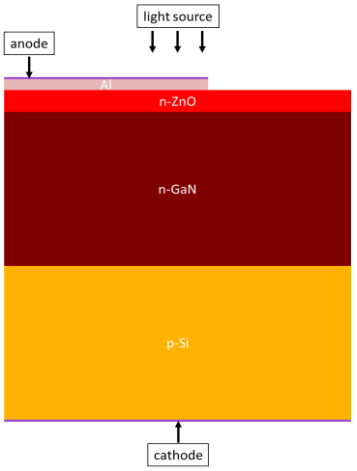


Fig 3. Simulation setup for optical illumination in ATLAS. The BEAM statement simulates incident light (0.3 μm–0.7 μm) applied from the top of the device to analyze spectral and I–V characteristics.

https://doi.org/10.24191/esteem.v21iSeptember.7129.g5014

## 3. RESULTS AND DISCUSSIONS

### 3.1 Device structure and doping profile

Fig. 4, Fig. 5, Fig. 6 and Fig. 7 show the simulated cross-sectional structures of ZnO/GaN and ZnO/PGaN photodetectors with varying ZnO thicknesses (0.1 µm, 0.5 µm, and 1.0 µm) and pore diameters (0.5 µm and 1.0 µm). The base structure consists of a p-type Si substrate, an n-type GaN layer (5 µm), and a ZnO layer of designated thickness. For ZnO/PGaN configurations, pores were introduced into the GaN layer prior to ZnO deposition, forming a vertically aligned porous interface. Aluminum electrodes were placed at the top-left and bottom surfaces as anode and cathode, respectively.

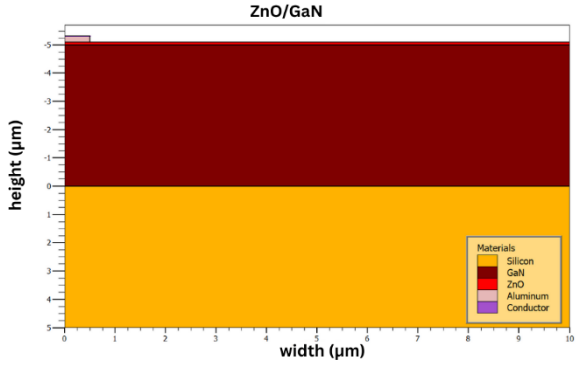


Fig 4. ZnO/GaN (0.1 µm ZnO Thickness) device structure.

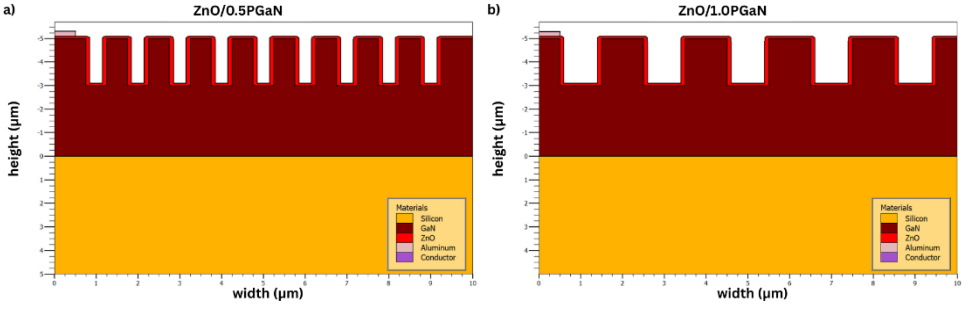


Fig 5. a) ZnO/PGaN (0.5 µm pore diameter) device structure. b)ZnO/PGaN (1.0 µm pore diameter) device structure.

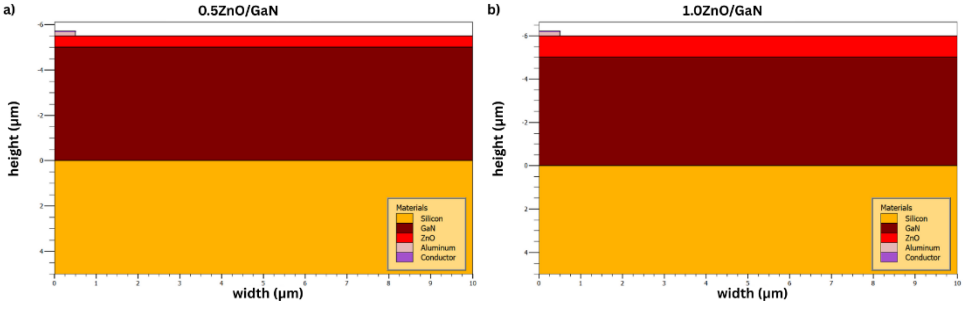


Fig 6. a) ZnO/GaN (0.5µm ZnO thickness) device structure. b) ZnO/GaN (1.0µm ZnO thickness) device structure.

https://doi.org/10.24191/esteem.v21iSeptember.7129.g5014

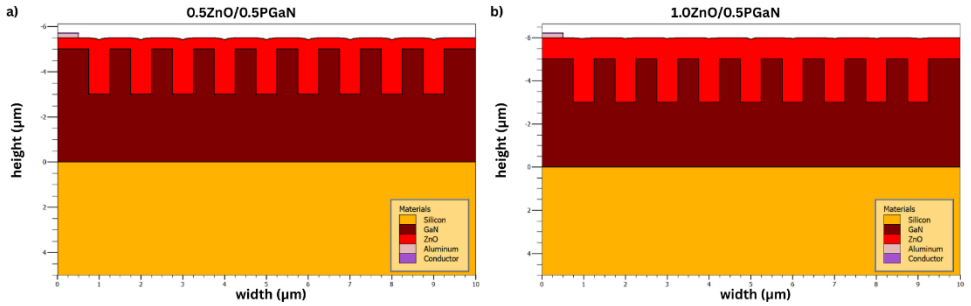


Fig 7. a) ZnO/PGaN (0.5 μm ZnO thickness) device structure. b) ZnO/PGaN (1.0 μm ZnO thickness) device structure.

Fig. 8 until Fig.14 present the corresponding doping profiles obtained from ATLAS for different structural configurations. All devices exhibit a consistent doping gradient, with the p-Si substrate heavily doped with boron, followed by the intrinsic or lightly n-doped GaN and ZnO layers. The doping profiles validate the successful formation of p–n heterojunctions in both ZnO/GaN and ZnO/PGaN devices. It is also evident that the introduction of pores did not alter the vertical doping gradient significantly, but could affect local electric field distributions and carrier recombination dynamics consistent with observations in similar nanostructured devices [5]. These structures serve as the foundation for analysing the electrical behaviour, specifically the I–V characteristics and current gain under dark and illuminated conditions.

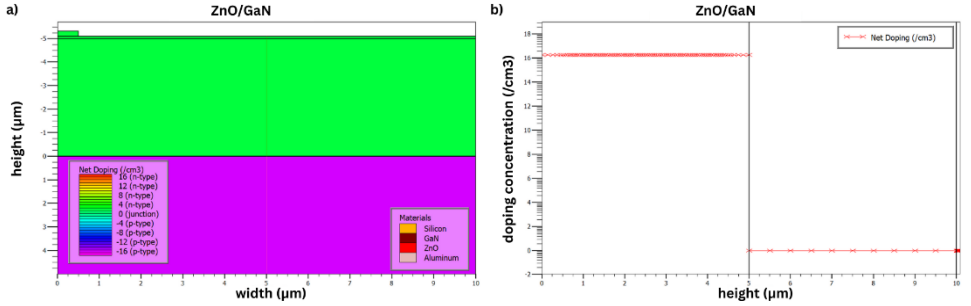


Fig 8. a) Net doping contour for ZnO/GaN (0.1 μm ZnO thickness). b) Net doping cutline for ZnO/GaN (0.1 μm ZnO thickness).

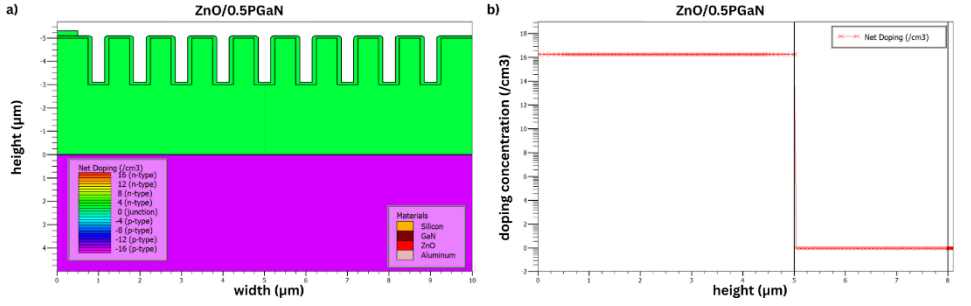


Fig 9. a) Net doping contour for ZnO/PGaN (0.5 μm pore diameter). b) Net doping cutline for ZnO/PGaN (0.5 μm pore diameter).

https://doi.org/10.24191/esteem.v21iSeptember.7129.g5014

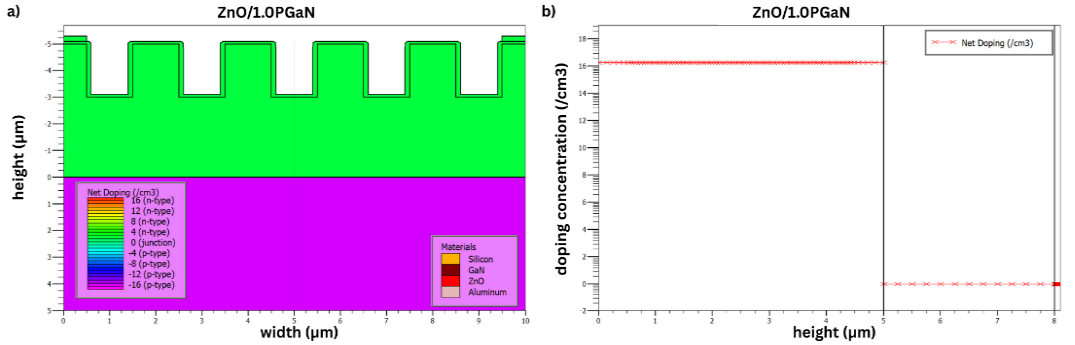


Fig 10. a) Net doping contour for ZnO/PGaN (1.0 μm pore diameter). b) Net doping cutline for ZnO/PGaN (1.0 μm pore diameter).

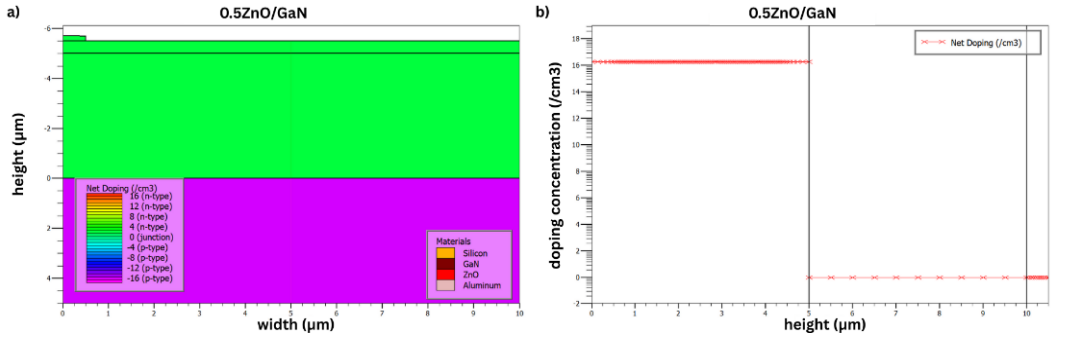


Fig 11. a) Net doping contour for ZnO/GaN (0.5 μm ZnO thickness). b) Net doping cutline for ZnO/GaN (0.5 μm ZnO thickness).

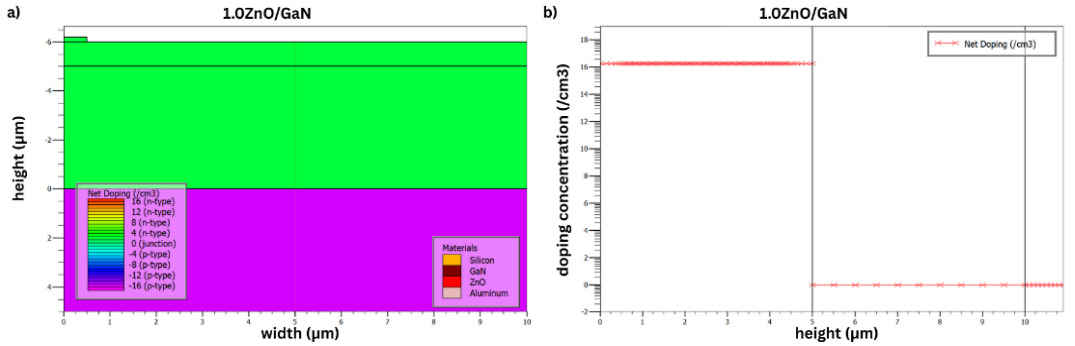


Fig 12. a) Net doping contour for ZnO/GaN (1.0 μm ZnO thickness). b) Net doping cutline for ZnO/GaN (1.0 μm ZnO thickness).

https://doi.org/10.24191/esteem.v21iSeptember.7129.g5014

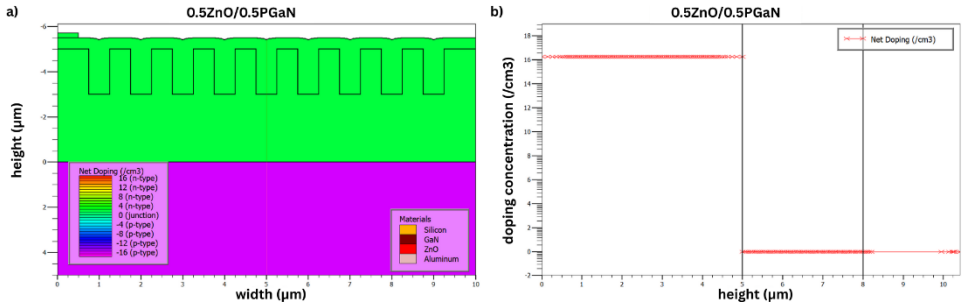


Fig 13. a) Net doping contour for ZnO/PGaN (0.5 µm ZnO thickness). b) Net doping cutline for ZnO/PGaN (0.5 µm ZnO thickness).

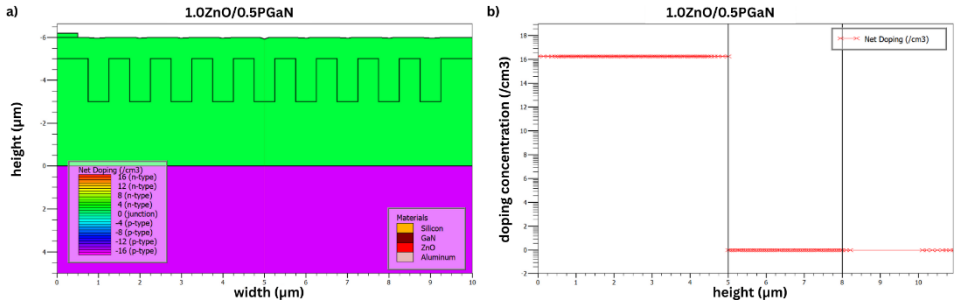


Fig 14. a) Net doping contour for ZnO/PGaN (1.0 µm ZnO thickness). b) Net doping cutline for ZnO/PGaN (1.0 µm ZnO thickness).

### 3.2 I-V characteristic and current gain analysis

The performance of the photodetectors was analysed through I–V measurements under both dark and illuminated conditions. The key metrics included photocurrent response and current gain, which was defined as the ratio of illuminated current to dark current.

*Effect of pore diameter (ZnO thickness fixed at 0.1 µm)*

Fig. 15 illustrates the I–V characteristics for ZnO/GaN and ZnO/PGaN devices with ZnO thickness fixed at 0.1 µm. The ZnO/PGaN device with a 0.5 µm pore diameter device exhibited the highest current gain approximately 4.7 times higher than the non-porous ZnO/GaN structure. This enhancement can be attributed to the increased light trapping and surface area provided by the porous architecture, which improves the photon absorption and carrier generation. Similar enhancements have been reported in UV photodetectors based on porous GaN integrated with ZnO, where nanostructured pores act as scattering centres and strain-relief buffers [3, 8]. The ZnO/PGaN with 0.5 µm pores exhibited higher current gain compared to 1.0 µm pores. This is attributed to stronger light scattering, larger surface-to-volume ratio, and shorter carrier diffusion paths, which together enhance the photon absorption and reduce the recombination losses [6, 10]. This observation is consistent with recent reports, where electrochemically etched GaN layers with finer pore structures exhibited enhanced carrier dynamics and optoelectronic performance [11, 18].

https://doi.org/10.24191/esteem.v21iSeptember.7129.g5014

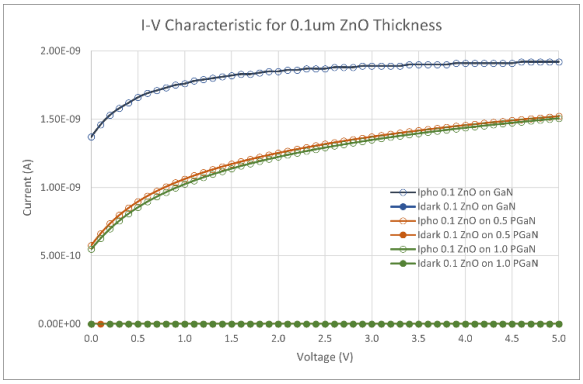


Fig 15. I-V Characteristics of ZnO/GaN and ZnO/PGaN for 0.1 µm ZnO thickness and different pore diameters.

Table 3. Current gain at 3.1 V for 0.1 µm ZnO thickness.

| Device | Pore Size (µm) | Current Gain |
|---|---|---|
| ZnO/GaN | N/A | $8.15 \times 10^8$ |
| ZnO/PGaN | 0.5 | $3.86 \times 10^9$ |
| ZnO/PGaN | 1.0 | $9.84 \times 10^8$ |

As shown in Table 3, the ZnO/PGaN with 0.5 µm pores achieved a current gain of $3.86 \times 10^9$, which is about 4.7 times higher than the non-porous ZnO/GaN device. This can be attributed to stronger photon scattering and larger effective surface area, which improve carrier generation. In contrast, the device with 1.0 µm pores shows a lower gain ($9.84 \times 10^8$), suggesting that excessively large pores reduce the light-trapping efficiency.

*Effect of ZnO thickness on ZnO/GaN*

Fig. 16 shows that increasing the ZnO thickness from 0.1 µm to 1.0 µm significantly increases the photocurrent and gain in ZnO/GaN devices. A thicker ZnO layer absorbs more incident photons, thereby generating more electron-hole pairs. This trend aligns with previous findings, in which tuning the ZnO film thickness improved light absorption and carrier transport efficiency in ZnO-based heterojunction photodetectors [9, 19].

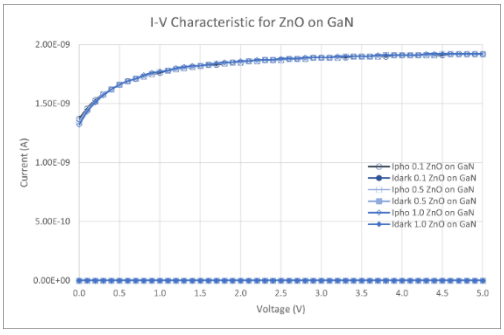


Fig 16. I-V characteristic of ZnO/GaN for different ZnO thicknesses.

https://doi.org/10.24191/esteem.v21iSeptember.7129.g5014

Table 4 demonstrates that increasing ZnO thickness from 0.1 µm to 1.0 µm enhances current gain from $5.92\times10^8$ to $9.13\times10^8$. This trend indicates that thicker ZnO layers absorb more photons, thereby producing higher electron-hole pair generation and improving the photocurrent. However, the improvement tends to saturate beyond 0.5 µm, indicating an optimal range for thickness.

Table 4. Current Gain at 3.3V for ZnO/GaN with varying ZnO thicknesses.

| ZnO Thickness (µm) | Current Gain |
|---|---|
| 0.1 | $5.92 \times 10^8$ |
| 0.5 | $8.56 \times 10^8$ |
| 1.0 | $9.13 \times 10^8$ |

*Effect of ZnO thickness on ZnO/PGaN (0.5µm pore diameter)*

Fig. 17 presents the I–V response for ZnO/PGaN devices with a fixed pore diameter (0.5 µm) and varied ZnO thicknesses. The 1.0 µm-thick ZnO layer achieved the highest current gain, confirming the synergistic effect of the porous architecture and active layer thickness on responsivity. The combination of high surface area from PGaN and optimised ZnO thickness significantly enhances light-matter interaction, consistent with recent simulations and experimental reports [6, 10].

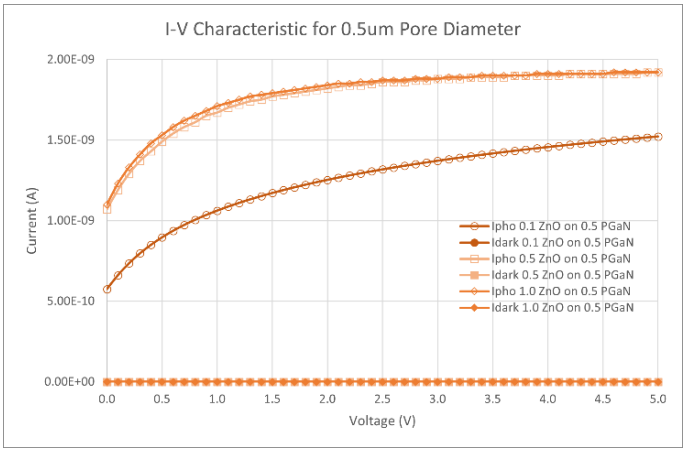


Fig 17. I-V characteristic of ZnO/PGaN for 0.5 µm pore diameter and different ZnO thicknesses.

From Table 5, there is evidence that the combination of porous GaN with 0.5 µm pores and thicker ZnO layers yields superior gain. The current gain increased from $2.65\times10^8$ (0.1 µm ZnO) to $1.47\times10^9$ (1.0 µm ZnO). This confirms a synergistic effect between pore-induced light scattering and enhanced absorption in thicker ZnO layers. Thus, ZnO/PGaN with 0.5 µm pores and 1.0 µm ZnO thickness provides the most promising structure for improved device responsivity

Table 5. Current gain at 2.0V for ZnO/PGaN (0.5 µm pore diameter).

| ZnO Thickness (µm) | Current Gain |
|---|---|
| 0.1 | $2.65 \times 10^8$ |
| 0.5 | $1.22 \times 10^9$ |
| 1.0 | $1.47 \times 10^9$ |

.

https://doi.org/10.24191/esteem.v21iSeptember.7129.g5014

These results support the conclusions of recent literature on porous-semiconductor-based photodetectors and highlight how nanostructural and thickness tuning can significantly enhance the optoelectronic device performance.

## 4. CONCLUSION

This study investigated the optoelectronic performance of ZnO/GaN and ZnO/PGaN photodetectors using SILVACO TCAD tools by varying the levels of ZnO thickness and PGaN pore diameter. The simulation results reveal that ZnO/PGaN structures exhibit significantly enhanced current gain compared to ZnO/GaN counterparts, mainly due to the suppressed dark current and improved light absorption via the increased surface area. Among the ZnO/PGaN configurations, a pore diameter of 0.5 μm demonstrated superior performance over 1.0 μm, suggesting that smaller pores facilitate better photoresponse. Additionally, increasing the ZnO thickness from 0.1 μm to 1.0 μm consistently improved the photocurrent gain in both GaN and porous GaN substrates, with the highest gain observed for ZnO/PGaN (0.5 μm pore, 1.0 μm ZnO). These findings confirm that both pore geometry and ZnO thickness are critical design parameters for optimising ZnO-based UV photodetectors. The simulation insights from this study may serve as a reference for future fabrication and optimisation of high-sensitivity, low dark-current optoelectronic devices.

## 5. ACKNOWLEDGEMENTS/FUNDING

The authors would like to express their sincere gratitude to Universiti Teknologi MARA, Penang Branch, particularly the Faculty of Electrical Engineering and the Department of Applied Sciences, for providing technical support and resources throughout the course of this research. Special thanks are also extended to the laboratory and simulation facilities staff members for their assistance, which contributed to the success of this study.

## 6. CONFLICT OF INTEREST STATEMENT

The authors declare that there is no conflict of interest regarding the publication of this paper. This research was conducted in the absence of any commercial, financial, or personal relationships that could be construed as a potential conflict of interest.

## 7. AUTHORS' CONTRIBUTIONS

**N. S. Mohd Hassan**: Investigation, formal analysis, methodology, writing original draft; **A. F. Abd Rahim**: Conceptualization, supervision, validation, writing review and editing; **N. S. Mohd Razali**: Software, simulation support (ATLAS), data curation; **R. Radzali** and **A. Mahmood**: Methodology advice, technical validation for GaN and PGaN simulations; **I. H. Hamzah** and **Z. Muhammad**: Writing, review and editing, data analysis; **M. F. Packeer Mohamed**: USM collaborator, Technical assistance on SILVACO TCAD tools.

## 8. REFERENCES

[1] L. Chu, C. Xu, W. Zeng, C. Nie, and Y. Hu, "Fabrication and Application of Different Nanostructured ZnO in Ultraviolet Photodetectors: A Review," *IEEE Sensors Journal*, vol. 22, no. 8, pp. 7451-7462, 2022. Available: https://doi.org/10.1109/JSEN.2022.3158650

https://doi.org/10.24191/esteem.v21iSeptember.7129.g5014

[2] T. Kente and S. D. Mhlanga, "Gallium nitride nanostructures: Synthesis, characterization and applications," *Journal of Crystal Growth*, vol. 444, pp. 55-72, 2016. Available: https://doi.org//10.1016/j.jcrysgro.2016.03.033

[3] L. Zhang et al., "One-step fabrication of porous GaN crystal membrane and its application in energy storage," *Scientific Reports,* vol. 7, no. 1, p. 44063, 2017. Available: https://doi.org/10.1038/srep44063

[4] D. Athow, "How GaN is changing the future of semiconductors," in TechRadar Pro, ed: *TechRadar*, 2022.

[5] D. Liu et al., "High-Performance Ultraviolet Photodetector Based on Graphene Quantum Dots Decorated ZnO Nanorods/GaN Film Isotype Heterojunctions," *Nanoscale Research Letters,* vol. 13, no. 1, p. 261, 2018. Available: https://doi.org/10.1186/s11671-018-2672-5

[6] R. Tang et al., "Ga2O3/GaN Heterostructural Ultraviolet Photodetectors with Exciton-Dominated Ultranarrow Response," *ACS Applied Electronic Materials*, vol. 4, no. 1, pp. 188-196, 2022. Available: https://doi.org/10.1021/acsaelm.1c00917

[7] F. K. Yam, Z. Hassan, and S. S. Ng, "Porous GaN prepared by UV assisted electrochemical etching," Thin Solid Films, vol. 515, no. 7, pp. 3469-3474, 2007. Available: https://doi.org/10.1016/j.tsf.2006.10.104

[8] C. Wang et al., "A ZnO/porous GaN heterojunction and its application as a humidity sensor," *Nanoscale Advances*, vol. 1, no. 3, pp. 1232-1239, 2019. Available: https://doi.org/10.1039/C8NA00243F

[9] S. Sharma, A. Sumathi, and C. Periasamy, "Photodetection Properties of ZnO/Si Heterojunction Diode: A Simulation Study," *IETE Technical Review*, vol. 34, no. 1, pp. 83-90, 2017. Available: https://doi.org/10.1080/02564602.2016.1145558

[10] W. Ouyang, F. Teng, J.-H. He, and X. Fang, "Enhancing the Photoelectric Performance of Photodetectors Based on Metal Oxide Semiconductors by Charge-Carrier Engineering," *Advanced Functional Materials,* vol. 29, no. 9, p. 1807672, 2019. Available: https://doi.org/10.1002/adfm.201807672

[11] H. Son, P. Uthirakumar, A. Y. Polyakov, J. H. Park, K. H. Lee, and I.-H. Lee, "Impact of porosity on the structural and optoelectronic properties of nanoporous GaN double layer fabricated via combined electrochemical and photoelectrochemical etching," *Applied Surface Science*, vol. 592, p. 153248, 2022. Available: https://doi.org/10.1016/j.apsusc.2022.153248

[12] H. Thaalbi et al., "Porous GaN Nanopyramids: Advancing Beyond Conventional Nanostructures for High-Brightness InGaN/GaN Quantum Wells Emission," *Advanced Functional Materials*, vol. 34, no. 41, p. 2406467, 2024. Available: https://doi.org/10.1002/adfm.202406467

[13] J. Wen et al., "High-Performance Ultraviolet Photodetectors Based on Nanoporous GaN with a Ga2O3 Single-Crystal Layer," *Nanomaterials*, vol. 14, no. 13, p. 1165, 2024. [Online]. Available: https://www.mdpi.com/2079-4991/14/13/1165

[14] M. Manoua et al., "Modeling and Optimization of n-ZnO/p-Si heterojunction using 2-dimensional numerical simulation," *Eur. Phys. J. Appl. Phys*., vol. 90, no. 1, p. 10101, 2020. [Online]. Available: https://doi.org/10.1051/epjap/2020190333

[15] G. Sabui, P. J. Parbrook, M. Arredondo-Arechavala, and Z. J. Shen, "Modeling and simulation of bulk gallium nitride power semiconductor devices," *AIP Advances*, vol. 6, no. 5, 2016. Available: https://doi.org/10.1063/1.4948794

[16] K. N. Tapily, "Synthesis of ALD Zinc Oxide and Thin Film Materials Optimization for UV Photodetector Applications," Doctor of Philosophy (PhD), *Electrical & Computer Engineering, Old Dominion University*, 2011. [Online]. Available: https://digitalcommons.odu.edu/ece_etds/124/

[17] A. Richter, S. W. Glunz, F. Werner, J. Schmidt, and A. Cuevas, "Improved quantitative description of Auger recombination in crystalline silicon," *Physical Review B*, vol. 86, no. 16, p. 165202, 2012. Available: https://doi.org/10.1103/PhysRevB.86.165202

https://doi.org/10.24191/esteem.v21iSeptember.7129.g5014

[18] J. Liu, J. Cui, and H. Xiao, "Electrochemical etching of n-type GaN in different electrolytes," *Journal of Alloys and Compounds*, vol. 983, p. 173846, 2024. Available: https://doi.org/10.1016/j.jallcom.2024.173846

[19] A. Janotti and C. G. Van de Walle, "Fundamentals of zinc oxide as a semiconductor," *Reports on Progress in Physics*, vol. 72, no. 12, p. 126501, 2009. Available: https://doi.org/10.1088/0034-4885/72/12/126501



https://doi.org/10.24191/esteem.v21iSeptember.7129.g5014